

Mössbauer Effect in Surface Studies: Fe⁵⁷ on W and on Ag†

J. W. BURTON* AND R. P. GODWIN‡

Department of Physics, University of Illinois, Urbana, Illinois

(Received 17 October 1966; revised manuscript received 10 February 1967)

The Mössbauer effect at crystal surfaces is discussed. Fe⁵⁷ on the surface of W and Ag has been measured under ultrahigh vacuum. The W experiment yielded Debye temperatures of 406±12, 354±30, and 255±30°K in the bulk, along the surface normal, and parallel to the surface, respectively. In Ag the bulk Debye temperature was 253±12°K while the surface value was 380±30°K and showed no angular dependence. Quadrupole splitting in both experiments indicated surface field gradients of about -3×10^{16} V/cm².

I. INTRODUCTION

CALCULATIONS of lattice-dynamical properties have recently been made on crystal models with free surfaces.¹⁻⁹ In the present work, the Mössbauer effect has been applied to surface investigations. It is useful because it is sensitive to lattice-binding forces, magnetic and electric fields, and the density of *s* electrons at the nucleus. Because of the difficulties encountered in surface-Mössbauer experiments only a few experiments have been attempted.¹⁰⁻¹²

In Sec. II the dynamics of surface atoms is presented with emphasis upon general features. In Sec. III we describe our experiments.

II. THEORY

A. Recoilless Fraction

The fraction *f* of gamma rays emitted without recoil is given in the harmonic approximation by¹³

$$f = \exp(-k^2 \langle x_\gamma^2 \rangle), \quad (1)$$

where $\langle x_\gamma^2 \rangle$ is the mean-square displacement (msd) of the emitting nucleus along the direction of the gamma and *k* is the magnitude of the gamma-wave vector. The

msd in a periodic crystal depends on the phonon frequency ω in the following way¹⁴

$$\langle x_\gamma^2 \rangle \propto \sum_\alpha [(\hat{\gamma} \cdot \hat{\epsilon}_\alpha)^2 / m\omega_\alpha] \coth(\frac{1}{2}\hbar\omega_\alpha\beta), \quad (2)$$

where α denotes phonon wave vector and polarization, $\beta = (k_B T)^{-1}$, *m* the atomic mass, and $\hat{\gamma}$ a unit vector in the direction of interest.

1. Einstein Model

Consider the high-temperature limit of Eq. (2). If we transform the sum to an integral, we find that all frequencies enter with equal weight. This result allows us to choose a single frequency that can be used to discuss the msd, hence the Einstein solid is a useful model. Since the high-temperature msd is inversely proportional to ω^2 , we can obtain an effective Einstein temperature from the Debye model as follows:

$$\frac{1}{\omega_E^2} = \left(\frac{1}{\omega^2} \right)_{av} = \left(\int_0^{\omega_m} d\omega / \int_0^{\omega_m} \omega^2 d\omega \right) = \frac{3}{\omega_m^2}. \quad (3)$$

This yields $\Theta_E = (1/\sqrt{3})\Theta_D$ where Θ_E and Θ_D are, respectively, Einstein and Debye temperatures. A similar calculation in the $T=0^\circ\text{K}$ limit yields $\Theta_E = \frac{2}{3}\Theta_m$. Visscher¹⁵ has verified numerically the Einstein model. We approximate a nucleus in a crystal by a particle of mass *m* bound in an oscillator potential with force constants K_1 , K_2 , and K_3 . For a one-dimensional oscillator in thermal equilibrium,

$$\langle x_i^2 \rangle = \frac{\hbar}{2m\omega_i} \coth(\frac{1}{2}\beta\hbar\omega_i) = \frac{\hbar^2}{2mk_B\Theta_i} \coth\left(\frac{1}{2}\frac{\Theta_i}{T}\right), \quad (4)$$

where $\omega_i = (K_i/m)^{1/2}$. If we expand the hyperbolic cotangent for high temperatures ($T \gtrsim \frac{1}{2}\Theta$)

$$\langle x_\gamma^2 \rangle \propto 1/\Theta_\gamma^2 \propto 1/K_\gamma, \quad (5)$$

where K_γ is the effective-force constant in the direction of the gamma. To apply this model we assume the force constants can be obtained by counting the bonds in the various directions. As an example, we consider a simple-cubic lattice and assume that nearest and next-nearest neighbors contribute equally to bind-

† This report is based on theses submitted in partial fulfillment of the requirements for the Ph.D. degree at the University of Illinois. The work described herein received support from the U.S. Air Force Office of Scientific Research under Contract AF 49(638)-1048.

* Present address: Carson-Newman College, Jefferson City, Tennessee.

‡ Present address: Deutsches Elektronen-Synchrotron, Hamburg, Germany.

¹ R. F. Wallis and D. C. Gazis, *Phys. Rev.* **128**, 106 (1962).

² M. Rich, *Phys. Letters* **4**, 153 (1963).

³ A. Corciovei and A. Berinde, *J. Phys. Radium* **24**, 89 (1963).

⁴ J. Cely, *Phys. Status Solidi* **4**, 521 (1964).

⁵ A. A. Maradudin and J. Melngailis, *Phys. Rev.* **133**, A1188 (1964).

⁶ R. F. Wallis, *Surface Sci.* **2**, 146 (1964).

⁷ B. C. Clark, R. Herman, and R. F. Wallis, *Phys. Rev.* **139**, A860 (1965).

⁸ F. O. Goodman, *Surface Sci.* **3**, 386 (1965).

⁹ J. R. Clem and R. P. Godwin, *Am. J. Phys.* **34**, 460 (1966).

¹⁰ F. G. Allen, *Bull. Am. Phys. Soc.* **9**, 296 (1964).

¹¹ P. A. Flinn, S. L. Ruby, and W. L. Kehl, *Science* **143**, 1434 (1964).

¹² B. J. Bowles and T. E. Cranshaw, *Phys. Letters* **17**, 258 (1965).

¹³ H. Frauenfelder, *The Mössbauer Effect* (W. A. Benjamin, Inc., New York, 1963).

¹⁴ D. Pines, *Elementary Excitations in Solids* (W. A. Benjamin, Inc., New York, 1963).

¹⁵ W. M. Visscher, *Phys. Rev.* **192**, 28 (1963).

ing but that bonds perpendicular to the direction of emission have no effect. In this approach the msd of a surface atom is anisotropic and greater perpendicular than parallel to the surface for an atom *in* the surface, while it is smaller perpendicular than parallel to the surface for an atom *on* the surface. The ratio of surface to bulk msd varies from 1.25 to 5 depending on site and direction.

2. Many-Body Approach

Clem and Godwin⁹ solved analytically for the msd in a one-dimensional chain with free ends. Clem¹⁶ pointed out that the one-dimensional eigenvectors may be used to obtain the qualitative behavior in three dimensions. Consider the high-temperature region. The msd of atom *i* is given by

$$\langle x_i^2 \rangle = (k_B T / m) \sum_{q, \lambda; \lambda=1,2,3} B_{q\lambda, i}^2 / \omega_{q, \lambda}^2 \quad (6)$$

where *q*, λ denote phonon wave vector and polarization, and $B_{q\lambda, i}$ an eigenvector of the normal-modes problem. For a one-dimensional lattice of *N* atoms with equilibrium spacing *a*⁹

$$B_{q, i} = (2/N)^{1/2} \cos[(i - \frac{1}{2})qa], \quad (7)$$

where $q = (j-1)\pi/Na$; $j = 2, 3, \dots, N$; and $i = 1, \dots, N$. We use this $B_{q, i}$ as a prototype. Assume linear dispersion so that $\omega \propto q$. With these assumptions

$$\langle x_i^2 \rangle \propto \sum (1/q^2) \cos^2[(i - \frac{1}{2})qz a], \quad (8)$$

where *z* is the direction of the surface normal. Transforming to an integral, we have

$$\begin{aligned} \langle x_i^2 \rangle &\propto \int_0^{a_m} \frac{q^2 dq}{q^2} \int_0^1 dy \cos^2[(i - \frac{1}{2})qay] \\ &= \frac{1}{2} q_m \left[1 + [(2i-1)q_m a]^{-1} \int_0^{u_m} \left(\frac{\sin u}{u} \right) du \right], \quad (9) \end{aligned}$$

where $y = \cos\theta$ and $u = (2i-1)qa$. The integral remain-

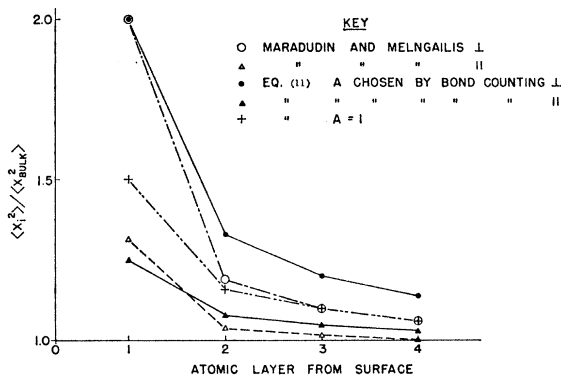


FIG. 1. Ratio of surface-atom to bulk-atom mean-square displacement.

¹⁶ J. R. Clem (private communication).

ing is the sine integral, $\text{Si}(u_m)$.¹⁷ We have then

$$\frac{\langle (x_i)^2 \rangle}{\langle (x_{\text{BULK}})^2 \rangle} = 1 + \frac{\text{Si}[(2i-1)q_m a]}{(2i-1)q_m a}. \quad (10)$$

If we assume $q_m = \pi/a$ (Brillouin-zone boundary) and note that $\text{Si}(u_m) \simeq \frac{1}{2}\pi$ for u_m of interest we expect that

$$\frac{\langle (x_{\gamma, i})^2 \rangle}{\langle (x_{\text{BULK}})^2 \rangle} \simeq 1 + \frac{A}{2(2i-1)}, \quad (11)$$

where *A* is a slowly varying function of order one. A similar calculation at $T=0^\circ\text{K}$ yields

$$\frac{\langle (x_{\gamma, i})^2 \rangle}{\langle (x_{\text{BULK}})^2 \rangle} \simeq 1 + \frac{4B}{\pi^2(2i-1)}, \quad (12)$$

with *B* of order one. Detailed calculations^{2-5,7,8} agree with the simple arguments. The model used by Maradudin and Melngailis⁵ is similar to the one we used in our "bond counting" discussion. In Fig. 1 we have plotted Maradudin's results and our Eq. (11).

B. Isomer Shift and Second-Order Doppler Shift

1. Isomer Shift

The isomer shift δE_I is given approximately by¹⁸

$$\delta E_I = \frac{2}{3} \pi Z e^2 [\langle r_B^2 \rangle - \langle r_A^2 \rangle] \{ |\Psi_a|^2 - |\Psi_e|^2 \}, \quad (13)$$

where *Ze* is the nuclear charge ($\langle r_B^2 \rangle$) and ($\langle r_A^2 \rangle$) are the root mean square radii of the nuclear-excited and ground states, and Ψ_a and Ψ_e are the electronic wave functions at the nucleus for the absorber and emitter, respectively. Anharmonicities in lattice binding are capable of introducing a linear-temperature dependence into the isomer shift. Suppose that the emitter nucleus has its average position changed slightly from its equilibrium position x_0 , we have then

$$\delta E_i = \delta E_I(x_0) - N \left. \frac{\partial |\Psi_e(x)|^2}{\partial x} \right|_{x_0} (x - x_0), \quad (14)$$

where *N* contains only nuclear parameters. Consider an atom bound in a Morse potential:

$$V(x) = U_0 \{ \exp[-2(x-x_0)/a] - 2 \exp[-(x-x_0)/a] \}. \quad (15)$$

For small displacements in the high-temperature regime the particle's average displacement is

$$\begin{aligned} \langle x - x_0 \rangle &\simeq \frac{\int_{-\infty}^{+\infty} y \exp[-\beta U_0 y^2 / a^2] (1 + y^2 / a^2) dy}{\int_{-\infty}^{+\infty} \exp[-\beta U_0 y^2 / a^2] dy} \\ &= \frac{3}{4} \frac{a}{U_0} k_B T, \quad (16) \end{aligned}$$

¹⁷ E. Jahnke and F. Emde, *Tables of Functions* (Dover Publications, Inc., New York, 1945).

where $y = x - x_0$. We require an expression for the electronic wave function and its spatial derivative. As a crude model, consider the wave function in the forbidden region outside a free-electron metal. The wave function is

$$\Psi(x) = \Psi(0) \exp[-(2m\Phi/\hbar^2)^{1/2}x] \equiv \Psi(0) \exp(-\alpha x), \quad (17)$$

where $\Psi(0)$ is the bulk wave function and Φ the work function. Equations (14), (16), and (17) yield

$$d(\delta E_T)/dT = N |\Psi(x_0)|^2 \frac{3}{2} (\alpha \alpha k_B / U_0). \quad (18)$$

With typical parameters and assuming $N |\Psi(x_0)|^2 \sim \delta E_T \sim 10^{-2}$ (typical for Fe^{57}) we find $d\delta E_T/dT \sim 10^{-5}$ cm/(sec deg). Since the temperature derivative of the Doppler shift for Fe^{57} is $\sim 6 \times 10^{-5}$ cm/(sec deg) effects of the type we discuss here may be measurable but will be difficult to identify.

2. Doppler Shift

The second-order Doppler shift δE_D is given by¹³

$$\delta E_D = (E/2c^2) \langle v^2 \rangle, \quad (19)$$

where E is the gamma energy and $\langle v^2 \rangle$ is the mean square velocity (msv) of the emitting nucleus. To calculate the msv we return to the oscillator model. We find

$$\langle v^2 \rangle = \sum_{i=1}^3 \langle v_i^2 \rangle = \frac{\hbar}{2m} \sum_{i=1}^3 \omega_i \coth(\frac{1}{2}\beta\hbar\omega_i). \quad (20)$$

In the high-temperature limit

$$\langle v^2 \rangle = (3k_B T/m) + (\hbar^2/12k_B T m) K_{\text{eff}}, \quad (21)$$

where $K_{\text{eff}} \equiv \sum K_i$.

Detailed calculations of the effects of free surfaces on the msv have been performed.^{1,5,9} "Bond counting" as well as a calculation by Maradudin and Melngailis,⁵ and an extension of their calculation by Burton¹⁸ find that for atoms in the bulk, *in* the surface, and *on* the surface of a simple-cubic lattice the magnitude of the quantum-correction term is in the approximate ratio 3:2:1.

C. Quadrupole Splitting

For a pure-quadrupole spectrum with axially-symmetric-field gradients the quadrupole shift δE_Q for Fe^{57} is given by¹³

$$\delta E_Q = \frac{1}{2} e\gamma (\partial^2 V / \partial z^2) Q, \quad (22)$$

where Q is the nuclear-quadrupole moment, $\partial^2 V / \partial z^2$ the electric-field gradient, and γ the Sternheimer anti-shielding factor. To estimate the field gradient, we suppose that a charge $-e$ is at a lattice spacing a above

the surface, simulating a missing positively charged ion. We then have

$$\partial^2 V / \partial z^2 = -(2e/a^3) \sim -10^{16} \text{ V/cm}^2. \quad (23)$$

This field gradient, along with an antishielding factor for Fe of about 15 and a quadrupole moment for the excited state of Fe^{57} of about 0.2 barn, yields a splitting of about the natural width of the Fe line. A study of the angular dependence of the intensities of a quadrupole-split line can give the direction of the field gradient.

III. EXPERIMENT

A. Introduction

Difficult technical problems must be solved to perform a quantitative surface Mössbauer experiment. First there is the problem of obtaining a clean surface. To obtain information that can be meaningfully interpreted experiments must be performed on single crystals. To avoid modifying our substrate and minimize interactions between adsorbed atoms we must work at low coverages. It is difficult to deposit material, even in ultrahigh vacuum, without introducing contamination. The small amount of activity requires long counting times. To minimize surface and bulk diffusion and island growth that may destroy surface effects and will certainly affect angular measurements, the sample should be cooled.

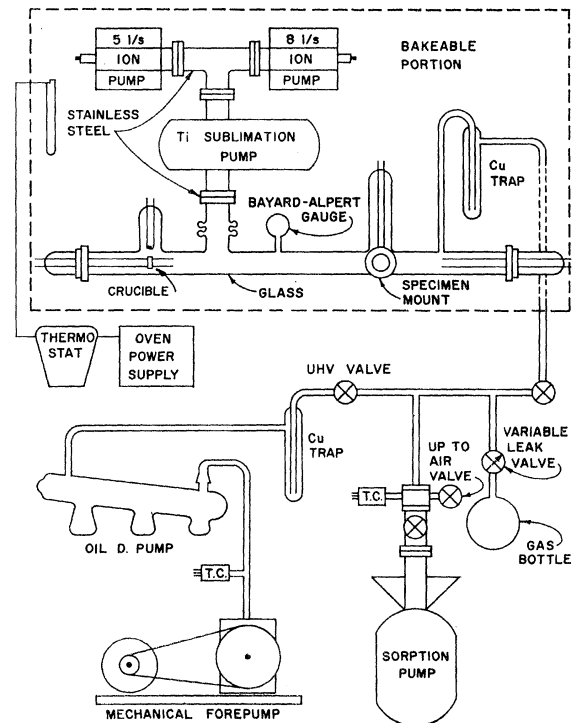


FIG. 2. Schematic representation of vacuum system.

¹⁸ J. W. Burton, Ph.D. thesis, University of Illinois, February, 1965 (unpublished).

B. Apparatus

1. Vacuum System

The systems reached pressures in the range of 10^{-10} Torr. They contained ion pumps as well as a water-cooled Ti pump. Figure 2 shows the system used in the Ag experiment, which is similar to the one used for W. Since the Mössbauer effect is sensitive to motion, the benches rode on vibration eliminators and the fore pumps were off during measurements.

2. Experimental Tube

A removable flange supported W feedthroughs upon which an Ohmically heated Mo crucible was mounted. The Ni-transfer vehicle supporting a Mo-foil-intermediate target could be slid onto the crucible supports and cleaned by electron bombardment. Figure 3 shows the portion of the tube in which the Mössbauer measurements were made.

The transfer target could be moved in front of the sample to deposit its radioactive source on the surface. The deposition was accomplished by heating the intermediate target with electron bombardment. A Ni-W thermocouple could be mounted on the sample for thermal calibration. A thinned window in the Pyrex tubing transmitted about 50% of the Fe^{57} 14-keV gamma rays. The target mount shown in Fig. 3 allowed both thermal and angular variation. Thermal contact between the bath and the target was established by screwing down a Cu disk mounted on a bellows.

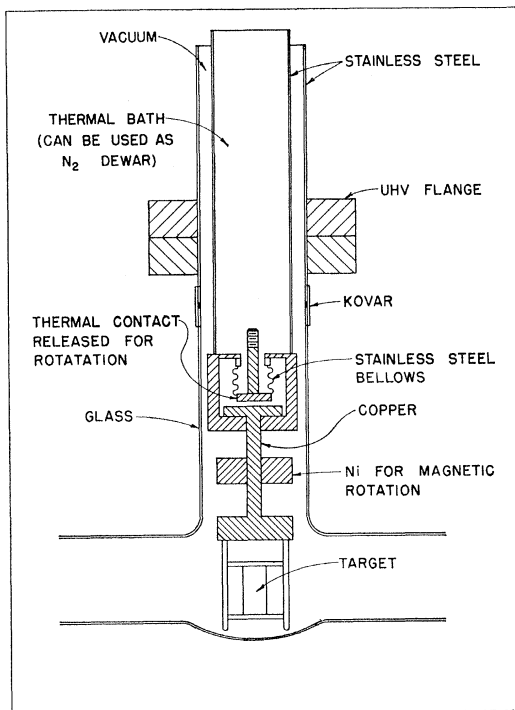


FIG. 3. Rotatable target mounting with temperature control.

3. Mössbauer Spectrometer

Electromechanical devices provided the drives.¹⁹⁻²¹ The counting system consisted of a Xe-filled proportional counter connected to a single-channel analyzer. A multichannel analyzer yielded a spectrum by sweeping through its channels storing 14-keV pulses as a function of velocity. The absorbers were of stainless steel enriched in Fe^{57} . They provided a single line with a width of 0.055 cm/sec. Calibrations were obtained by measuring the line splitting of Fe^{57} in iron.

C. Procedure and Results

1. Iron in and on Tungsten

To prepare a source of Co^{57} in W, a solution of $CoCl$ was dried onto a W ribbon, reduced in H_2 at $850^\circ C$ and then heated to about $2000^\circ C$ in H_2 .

The initial spectra consisted of a predominate single peak, plus the six-line spectrum of Fe^{57} in Co weakly superimposed. After etching the source in HNO_3 the single line remained. When heated, the Co apparently had collected into islands on the surface, as well as diffused into the bulk. The single-line spectrum was studied at 80, 300, and $500^\circ K$. The results are in agreement with those obtained by Schiffer, Parks, and Heberle.²²

For the surface experiment, a 0.25-mm sheet of polycrystalline W was prepared by electropolishing away 0.1 mm in NaOH. 0.2 mCi of Co^{57} was dried onto a ribbon of W, reduced in H_2 , and inserted into the system. The substrate and intermediate target were cleaned by heating to $2000^\circ C$ at pressures of 10^{-7} Torr and less. The crucible was outgassed at $900^\circ C$ and flashed to $1200^\circ C$ (threshold for evaporation of Co). After cooling the substrate to $100^\circ K$, the activity was evaporated onto the intermediate target and then the substrate. The pressure rose briefly to about 10^{-7} Torr during evaporation and remained below 10^{-9} Torr during the remainder of the experiment.

Spectra were measured with the source at $100^\circ K$, and angles of 0° and 60° , measured from the surface normal. Then the source was heated briefly to some temperature between 300° and $500^\circ K$. Measurements were made at 100 to $500^\circ K$ following the heating. The source was then heated to several higher temperatures, up to $1200^\circ K$. After each heating, the source was cooled to $500^\circ K$ for measurements. Finally, the source was cooled to $300^\circ K$, and to $100^\circ K$, for measurements.

The spectra obtained consist of a broad asymmetric line. Typical spectra are shown in Fig. 4. A least-

¹⁹ R. L. Cohen, P. G. McMullin, and G. K. Wertheim, *Rev. Sci. Instr.* **34**, 671 (1963).

²⁰ F. C. Ruegg, J. J. Spijkermann, and J. R. DeVoe, *Rev. Sci. Instr.* **36**, 356 (1965).

²¹ G. K. Wertheim and R. L. Cohen, in *Applications of the Mössbauer Effect in Chemistry and Solid-State Physics* (International Atomic Energy Agency, Vienna, 1966), p. 48.

²² J. P. Schiffer, P. N. Parks, and J. Heberle, *Phys. Rev.* **133**, A1553 (1964).

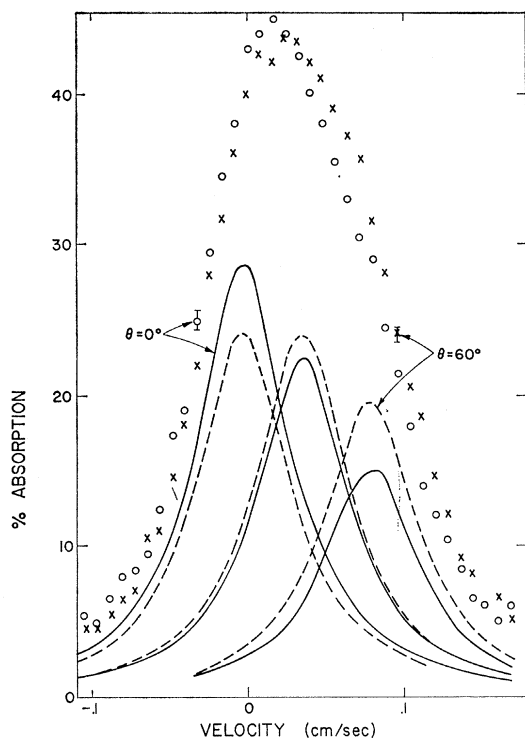


FIG. 4. Mössbauer spectra on polycrystalline W, at 100°K.

squares fit¹⁸ indicates that the line has three components. The intensity and position of the middle line agree with those of the spectra taken with Co in the bulk of W. Hence it was assumed that the center line is due to atoms which had diffused into the bulk and that the two outer lines were due to surface effects.

At each temperature, the spectra for both angles were fitted simultaneously. The positions and widths were constrained to be the same for both angles, but the intensities were allowed to be independent of the angle. The intensity data were normalized so that the intensity of the middle line was the same for both angles. Debye temperatures were found from the slope of a linear fit of the logarithm of the intensity parameters versus temperature. The intensity parameters were normalized to agree with the calculated Debye-Waller factor at 300°K. The results are plotted in Fig. 5.

The Debye temperature thus obtained for the bulk is $406 \pm 12^\circ\text{K}$. The intensity parameters for the middle line of the surface spectra yielded an effective Debye temperature of $400 \pm 70^\circ\text{K}$ while the outer lines yielded Debye temperatures of $340 \pm 30^\circ\text{K}$ at the 0° angle, and $273 \pm 30^\circ\text{K}$ at the 60° angle. The results reflect an average over the solid angle of the detector. The effective Debye temperature on the surface was deduced to be $354 \pm 30^\circ\text{K}$ along the normal and $255 \pm 30^\circ\text{K}$ parallel to the surface.

From the Debye temperatures, the ratio between the msd of the atom on the surface and that of the bulk is found to be 1.3 ± 0.2 along the normal and

2.5 ± 0.3 parallel to the surface. The simple model presented earlier predicts ratios of 1.4 and 2.3, respectively, for atoms bound above the top layer of the substrate. Hence, it appears that the nucleus is bound above the surface.

The middle line at 300°K is shifted 0.0268 ± 0.0014 cm/sec in the positive-energy direction with respect to our stainless steel absorber. (The Fe⁵⁷-in-iron calibration spectrum is shifted 0.0088 cm/sec above the absorber.) The temperature gradient of the position of the middle line is $-(5.7 \pm 0.6) \times 10^{-5}$ cm/sec °K. The position of the bulk line is 0.0239 ± 0.0002 cm/sec, with a temperature gradient of $-(6.35 \pm 0.15) \times 10^{-5}$ cm/sec °K.

The upper surface line is shifted by 0.0658 ± 0.0011 cm/sec at 300°K, with a temperature gradient of $-(6.0 \pm 0.6) \times 10^{-5}$ cm/sec °K. The lower line is shifted by -0.0123 ± 0.0010 cm/sec, with a temperature gradient of $-(5.3 \pm 0.6) \times 10^{-5}$ cm/sec °K. At 300°K the splitting of the two surface lines is 0.078 ± 0.002 cm/sec, indicating the field gradient due to the surface is about -2.4×10^{16} V/cm². The average width of the lines is 0.0669 ± 0.0005 cm/sec.

The average ratio of the intensities of the two surface lines is 2.06 ± 0.07 at 0° , and 1.38 ± 0.06 at 60° . The expected range of this ratio is 1.9–2.5 at 0° , and 0.91–1.02 at 60° , based on the angular correlation of quadrupole-split lines and the counter geometry. The lower line is most intense, implying it corresponds to the transition from the $m = \pm \frac{3}{2}$ state and that the field gradient is negative.

Discrepancies in the experiment can be primarily attributed to systematic errors introduced in the fitting of unresolved lines. Deviations of the line shape from the assumed Breit-Wigner would cause a small systematic error in the middle line and larger errors in the two outer lines.

An attempt was made to repeat the experiment, using the (310) surface of a single crystal slab of W.²³

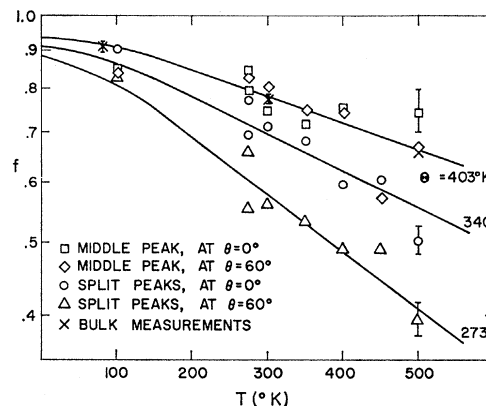


FIG. 5. Recoilless fraction versus temperature. Line represents the best fit to the Debye-Waller formula.

²³ We thank Dr. F. Propst and G. Tibbetts for the tungsten sample.

Typical spectra are shown in Fig. 6. The asymmetry of the lines is more apparent than on the polycrystalline substrate. The computer analysis revealed two lines, of width 0.081 ± 0.002 cm/sec and split by 0.067 ± 0.002 cm/sec. The absence of grain boundaries apparently reduced the diffusion into the bulk, practically eliminating the middle line. The splitting in the single-crystal experiment yields a value of -2.1×10^{16} V/cm² for the surface field gradient.

In the single-crystal experiment, technical difficulties rendered the angular dependence unreliable, although the results qualitatively agree with the earlier work. Upon heating, additional lines were observed in the spectrum, indicating that oxidation had taken place.

A restudy of the polycrystalline spectra showed some evidence of oxidation also. In the polycrystalline experiment, the pressure bursts accompanying the heatings were less, apparently causing less oxidation.

2. Iron in and on Silver

A single crystal of Ag²⁴ was sawed into slabs 1.5-mm thick. Visible scratches were removed with polishing paper. An electropolish (solution: 35 gm/liter AgCN, 37 gm/liter KCN, and 38 gm/liter K₂CO₃) removed 0.7 mm from the surface. The crystal was then etched for several seconds in 55% by volume of HNO₃ in distilled H₂O. Farnsworth²⁵ and Webb²⁶ have demonstrated that this treatment prepares good surfaces. One slab was examined with a reflection x ray. The normal to the crystal face was within several degrees of a [100] direction and little mosaic dispersion was present.

To prepare the Fe-in-Ag sample 0.09 mCi of ⁵⁷Co²⁷ was plated onto one of the Ag slabs. Following Kitchens *et al.*²⁸ the Co was diffused in by heating at 900°C for two hours. The silver recrystallized over about 25% of its cross section.

Spectra yielded a single symmetric line of width (0.051 ± 0.002) cm/sec. The line shifts with respect to ⁵⁷Fe in iron were (0.072 ± 0.002) , (0.056 ± 0.002) , and (0.050 ± 0.002) cm/sec at temperatures of 90, 295, and 380°K, respectively. The dependence of the resonance dip on temperature yielded an effective Debye temperature[†] of (253 ± 12) °K. The temperature dependence of the line position was $-(7.5 \pm 0.5) \times 10^{-5}$ cm/(sec deg).

The position of our line agreed with that of Kitchens *et al.*²⁸ They found a Debye temperature from the Doppler shift of 270°K. Low-energy electron diffraction²⁶

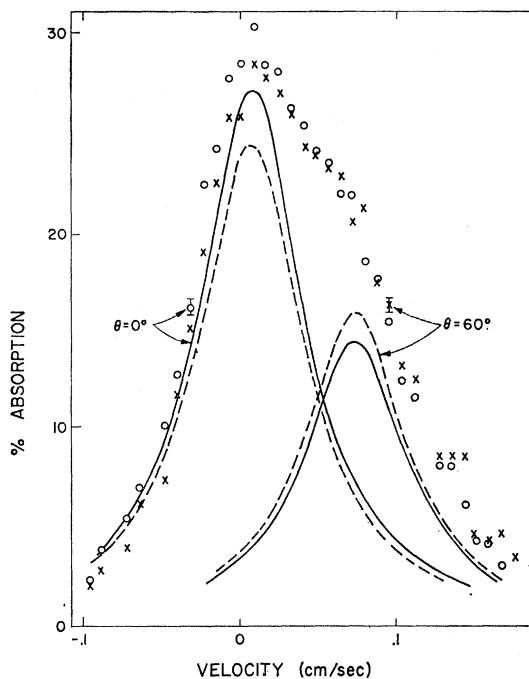


FIG. 6. Mössbauer spectra on single-crystal W at 80°K.

(LEED) and specific-heat measurements yield Debye temperatures of 210 and 225°K, respectively, for pure Ag.

For the Fe-on-Ag experiment one of the single crystal slabs was used as the substrate. Special care was taken to avoid recrystallization. 0.2 mCi of ⁵⁷Co was plated onto a W wire which had been outgassed in vacuum. The Co was reduced in H₂ and then diffused into the wire.

After insertion of the activity a system pressure of 2×10^{-10} Torr was obtained. The transfer foil and crucible were outgassed at 1200 and 900°C, respectively, for several hours. The Ag crystal was then outgassed at 800–850°C for 15 min. The carrier foil and Ag target were outgassed until the pressure in the system remained less than 5×10^{-9} Torr with the carrier foil at 1200°C and the Ag slab at an estimated 850°C. The sample was evaporated onto the transfer foil. Thermal equilibrium between the crystal and liquid-N₂ bath was established and the radioactive isotope evaporated onto the Ag surface. Although only about one-tenth of the activity was deposited upon the Ag virtually no "lost" activity was in the vicinity of the sample. After each Mössbauer run the Ti pump and Bayard-Alpert gauge were operated. The pressure was held to 5×10^{-10} Torr.

The spectra obtained consisted of a broad asymmetric line. No angular dependence was observed. The data were first fit to a single Lorentzian peak. The single-line fit yielded a width of (0.108 ± 0.002) cm/sec. The position of the line with respect to Fe-in-Fe was

²⁴ We thank Professor Lazarus for the silver crystal and R. Hinton of the Metallurgy Department at Illinois for aid in sample preparation.

²⁵ H. E. Farnsworth, Phys. Rev. **40**, 684 (1932).

²⁶ M. B. Webb, E. R. Jones, and J. T. McKinney, Bull. Am. Phys. Soc. **10**, 1105 (1965) and private communication.

²⁷ We thank Oak Ridge National Laboratory for the high specific activity cobalt (ratio Co⁵⁷/Co⁵⁹ of about 3/1 claimed).

²⁸ T. A. Kitchens, W. A. Steyert, and R. D. Taylor, Phys. Rev. **138**, A467 (1965).

$(13.2 \pm 0.9) \times 10^{-3}$, $(5.8 \pm 1.9) \times 10^{-3}$, $(1.4 \pm 0.9) \times 10^{-3}$, and $-(0.5 \pm 1.0) \times 10^{-3}$ cm/sec for temperatures of 93, 223, 293, and 373°K, respectively. The temperature dependence of the line position was $-(5.1 \pm 0.6) \times 10^{-5}$ cm/sec. deg. Area measurements yielded an effective Debye temperature of (380 ± 30) °K. A fit to two peaks of equal width yielded lines of width (0.083 ± 0.002) cm/sec split by (0.044 ± 0.001) cm/sec. An χ^2 test yielded higher confidence levels for the two-line fits. The ratio of the area of the larger to that of the smaller line was (1.4 ± 0.2) , (1.5 ± 0.2) , (1.8 ± 0.4) , and (2.4 ± 0.8) at temperatures of 93, 223, and 373°K, respectively. The Debye temperature of the two-line fit was (360 ± 15) °K.

The sample was returned to low temperatures and spectra obtained. The results reproduced the earlier spectra. A spectrum was run at room temperature after several days exposure to the atmosphere. The line had broadened by approximately 15% on the positive-velocity side.

A measurement of the radioisotope on the sample indicated that the activity was quite uniformly distributed.

The lack of angular dependence was disappointing. Two plausible reasons for the absence of angular dependence are that the surface was not well prepared or that the Co collected in islands. The isomer shift observed was different from that observed for Fe-in-Ag and near zero. The Debye temperature of (380 ± 30) °K for surface atoms is difficult to correlate with the bulk value of about 260°K since theory predicts a surface Debye temperature of about $1/\sqrt{2}$ the bulk value. The Debye temperature found in the surface measurement was suspiciously near that in bulk Co or Fe.

An analysis of the asymmetric line as two-quadrupole-split lines implies a field gradient normal to the surface of about -3×10^{16} V/cm².

The temperature dependence of the line position was smaller than that measured in the bulk-silver experiment. The change could have been due to the second-order Doppler effect for surface atoms or to the isomer shift of surface atoms.

IV. DISCUSSION

Our work and the previous Mössbauer surface studies have yielded meager information. We were particularly

interested in measuring the Debye temperatures for surface atoms relative to those for bulk atoms. No meaningful pattern has come to light. Allen¹⁰ found surface and bulk Debye temperatures essentially equal for Fe *on* and *in* Si. Our spectra for Fe *on* and *in* W indicated surface Debye temperatures were less than those of the bulk and showed an angular dependence in accord with simple theories. With Fe *in* and *on* Ag we found higher Debye temperatures for surface atoms than for bulk atoms. An extension of the work of Marshall and Wilenzick²⁹ on size effects in small Au crystals may be helpful.

The temperature dependence of the line position should be given careful study. The low-counting rates and broadened lines found in the experiments make it difficult to measure resonance areas and thus Debye temperatures. Measurements of the line positions from low to high temperatures can give Debye temperatures from the Doppler shift and possibly also show evidence of binding anharmonicities through the isomer shift. All the experiments performed thus far appear to give evidence of surface effects on the temperature dependence of the line position.

The quadrupole-splitting analysis in our experiments is not clean. It may be possible with a magnetically-polarized absorber to obtain (at the cost of decreasing already low-counting rates) better information upon the electric-field gradients.

A systematic study of surfaces will not be easy. Iron is a very difficult material to work with because it is difficult to purify and is easily oxidized. The ideal experiment from a theoretical standpoint would be Fe⁵⁷ on Fe. Unfortunately Fe⁵⁷ is apparently the only isotope suitable for experiments with the present techniques.

Note added in Proof: A review of this and related problems has recently been published. See A. A. Maradudin, *Solid State Phys.* **19**, 100 (1966).

ACKNOWLEDGMENTS

The authors wish to recognize the guidance of Professor H. Frauenfelder, the advice of Professor P. Debrunner, and the technical assistance of J. Culton.

²⁹ S. W. Marshall and R. M. Wilenzick, *Phys. Rev. Letters* **16**, 219 (1966).